Supplementary Information

Present-day warm pool constrains future tropical precipitation

[1]In-Hong Park, [1]Sang-Wook Yeh[*], [2]Seung-Ki Min, [3]Yoo-Geun Ham and [4]Ben P. Kirtman

[1] Department of Marine Science and Convergence Engineering, Hanyang University, ERICA, Ansan, Republic of Korea.

[2] Division of Environmental Science and Engineering, Pohang University of Science and Technology, Pohang, Gyeongbuk, Republic of Korea.

[3] Department of Oceanography, Chonnam National University, Gwangju, Republic of Korea.

[4] Rosenstiel School for Marine and Atmospheric Science, University of Miami, Miami, FL, USA.

[*]*Corresponding author: Prof. Sang-Wook Yeh (e-mail: swyeh@hanyang.ac.kr, South Korea, Hanyang University.)*

Submitted to Communications Earth & Environment

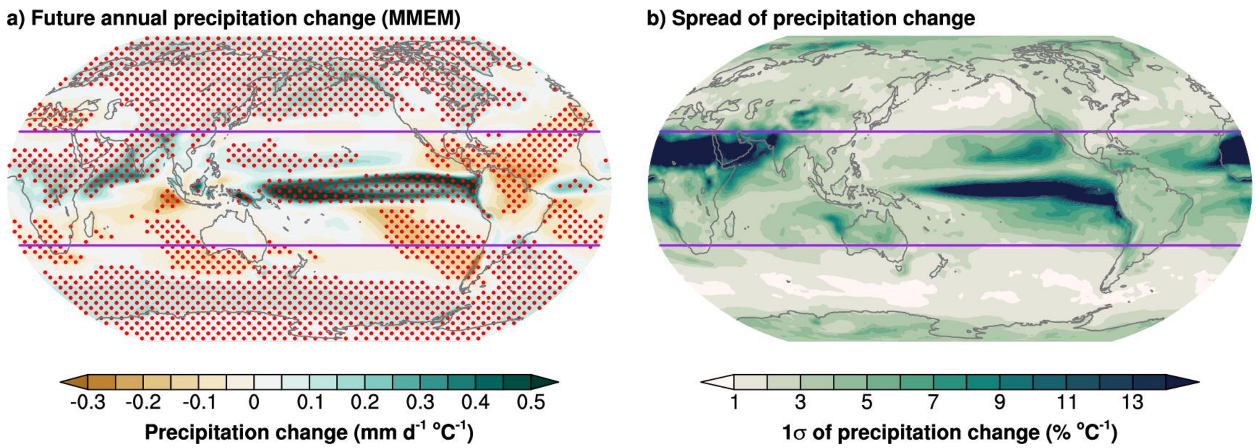

Supplementary Figure 1. Inter-model consistency and uncertainty of future global annual precipitation changes from 38 CMIP6 models. a) Projected precipitation changes (shading) and area of high model consistency. Red stipples illustrate the area where same sign of changes in CMIP6 (> 80% , 31 of total 38 models). **b)** Inter-model spread (one-standard deviation) of projected precipitation changes among CMIP6 models. Units are percent (%) for comparing relative changes among models. Purple horizontal lines illustrate the tropical boundary (30°S–30°N). Precipitation is normalized through dividing by the global mean surface temperature anomalies of each model.

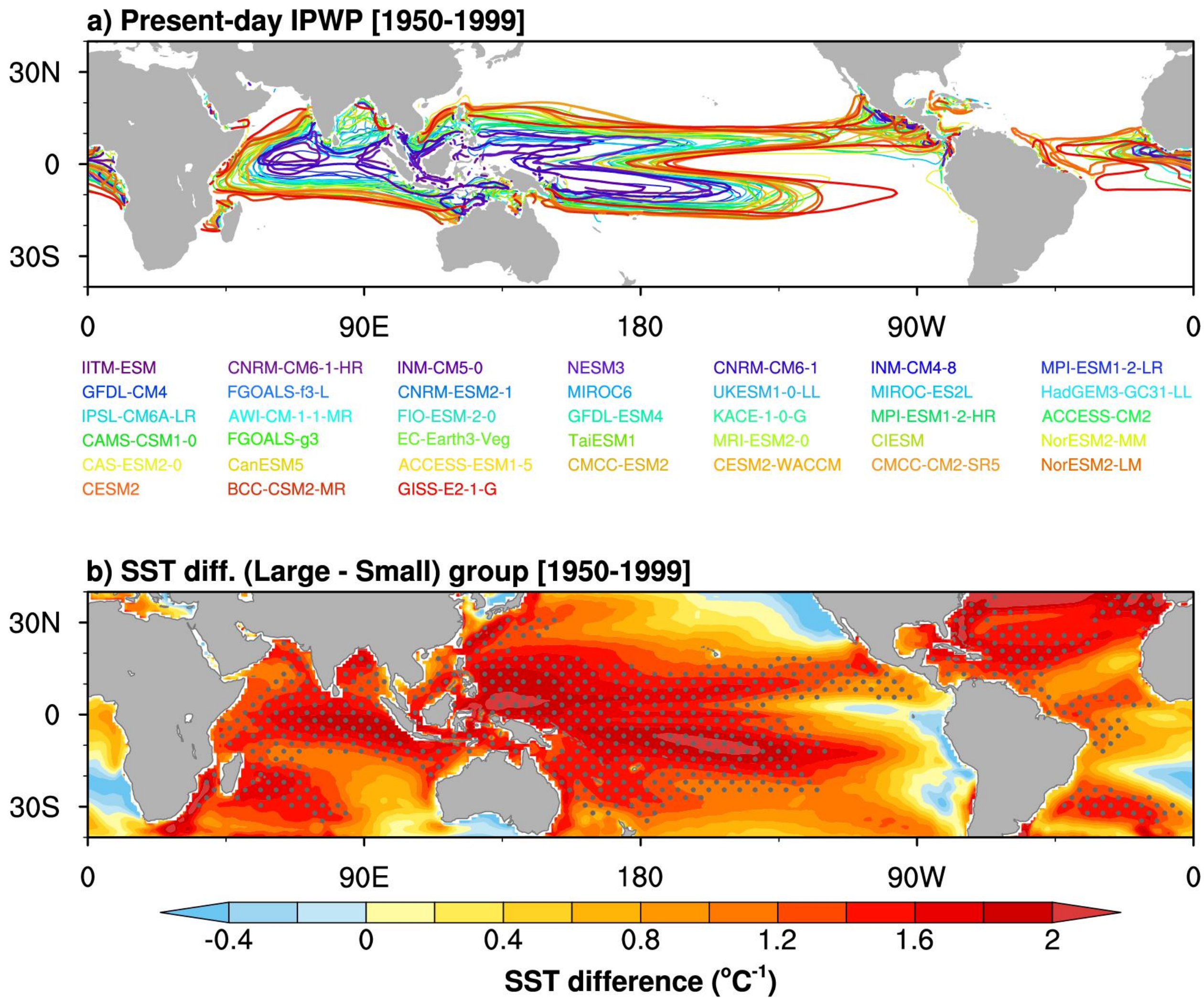

Supplementary Figure 2. Warm pool area of 38 CMIP6 models and SST difference from average of 5-models with largest IPWP size minus average of 5-models with smallest IPWP size in the present-day. a) Tropical warm pool area (SST > 28℃) of each model from small IPWP size models (blue) to large IPWP size models (red). **b)** SST difference between 5-models with largest IPWP size and 5-models with smallest IPWP size in the preset-day. Stipples indicates the area where SST difference is significant at the 99% confidence level using student t-test.

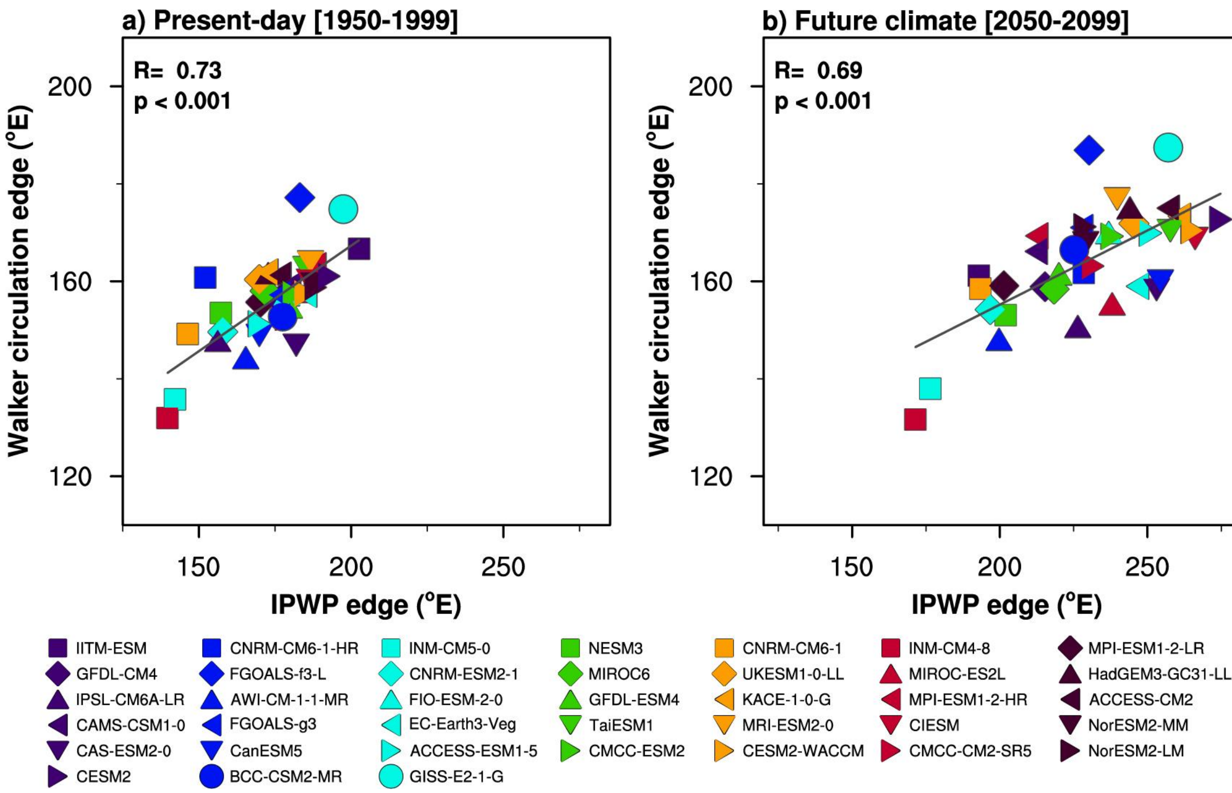

Supplementary Figure 3. Correlation between eastern edge of the IPWP and western edge of the Walker circulation's branch in a) the present-day and b) future climate.

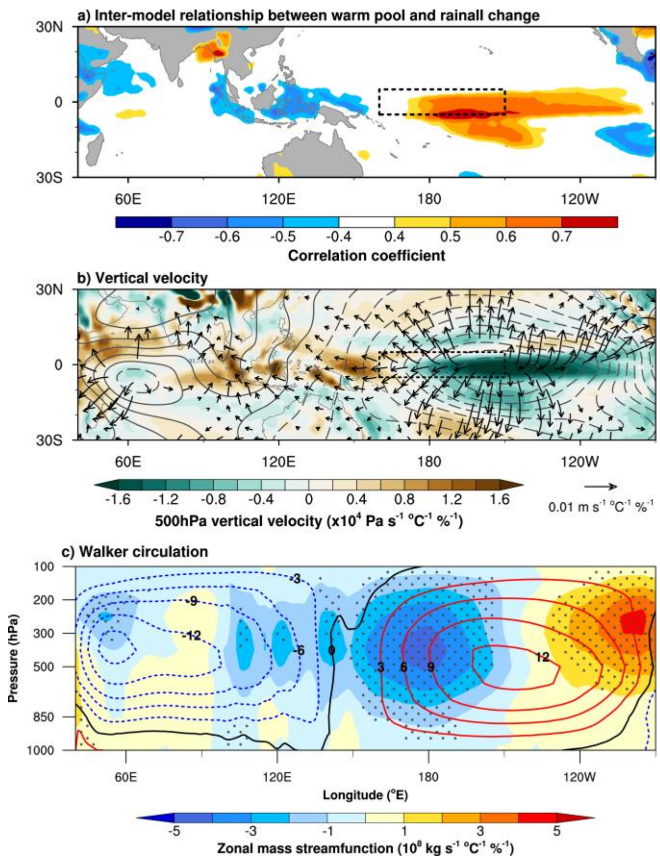

Supplementary Figure 4. Inter-model relationship and regressions of projected changes under RCP8.5 onto the present-day IPWP size from 26 CMIP5 models. a) Inter-model correlations between projected precipitation changes and the present-day IPWP size among CMIP5 models. Shading indicates the statistically significant size at a 95% confidence level in a student t-test. Dashed boxes denote the CETP (5°S–5°N, 160°E–150°W, same as Niño 4). **b)** Regressed future changes in 500hPa vertical velocity ($\times 10^4$ Pa s^{-1}, the upward motion is negative), 200hPa velocity potential (contour interval: 0.3×10^3 s^{-1}), and divergent wind (vectors, m s^{-1}). **c)** Regressed future changes in zonal stream function (shading, 10^8 kg s^{-1}) along the equator (5°S–5°N mean). Contours indicate MME mean of zonal stream function (10^{10} kg s^{-1}) in the present-day (1950–1999). Stipples indicate regions of significance at the 95% confidence level in a t-test.

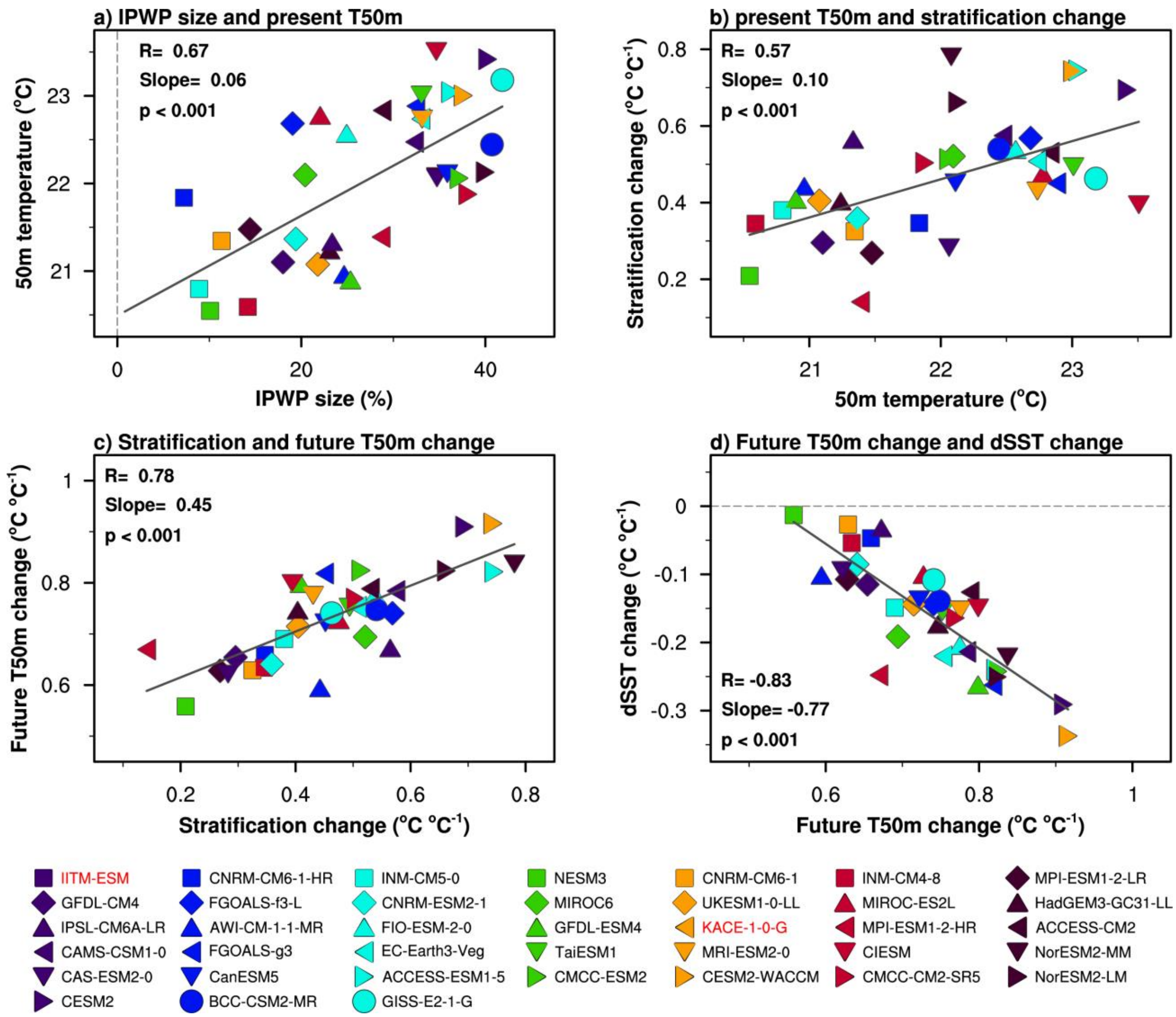

Supplementary Figure 5. Inter-model correlation of future zonal SST gradient anomaly against the IPWP size in the present under SSP5-8.5 among CMIP6 CGCMs. a) Simulated IPWP size (%) in the present-day versus the average temperature (℃) of the upper 50 m of the ocean in the eastern Pacific during the present-day. **b)** Upper 50 m ocean mean temperature in the present-day over the eastern Pacific versus future anomalies of ocean stratification, defined as upper 50 m mean temperature minus 150 m ocean temperature in the eastern Pacific (℃). **c)** The future anomaly of ocean stratification in the Eastern Pacific versus future anomaly of the upper 50 m ocean temperature (℃). **d)** The future anomaly of the upper 50 m ocean temperature versus that of the zonal SST gradient (western Pacific minus eastern Pacific). The inter-model correlation coefficients (r) displayed in each panel are statistically significant at the 99% confidence level. Models with a red label do not provide potential ocean temperature.

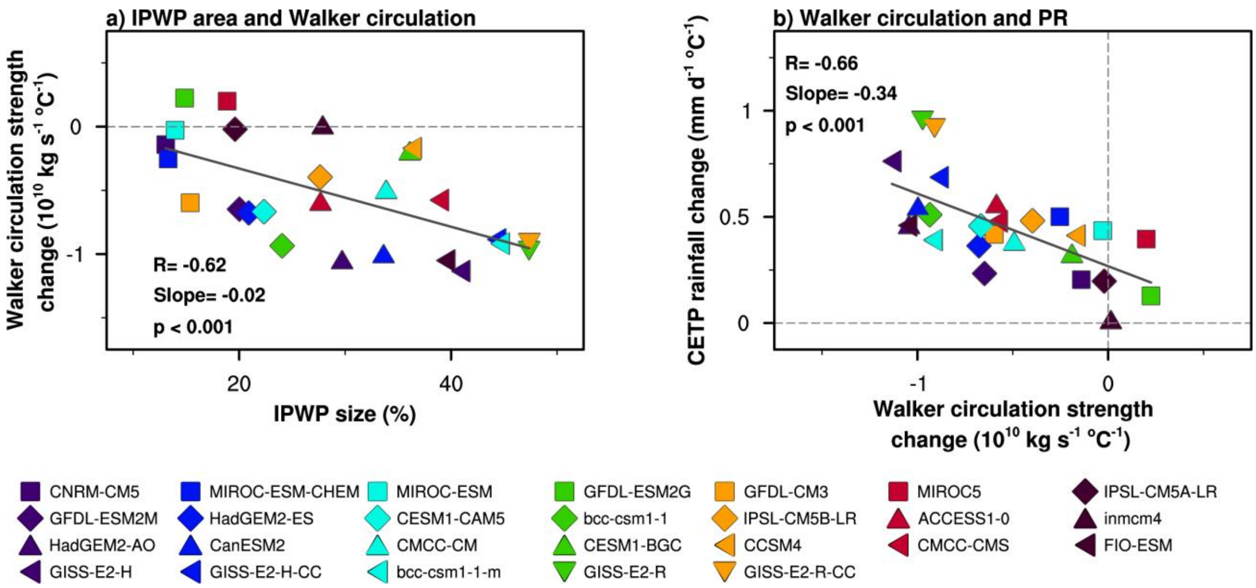

Supplementary Figure 6. Inter-model relationship between the present-day IPWP size and future projections in RCP-8.5 among CMIP5 CGCMs. a) Simulated IPWP size (%) in the present-day versus future change in Walker circulation strength (10^{10} kg s^{-1}). **b)** Future of Walker circulation strength versus that of Central Pacific precipitation (mm day^{-1}, 5°S–5°N, 160°E–150°W). The inter-model correlation coefficients (r), slope and p-value are displayed in each panel are statistically significant at the 99% confidence level.

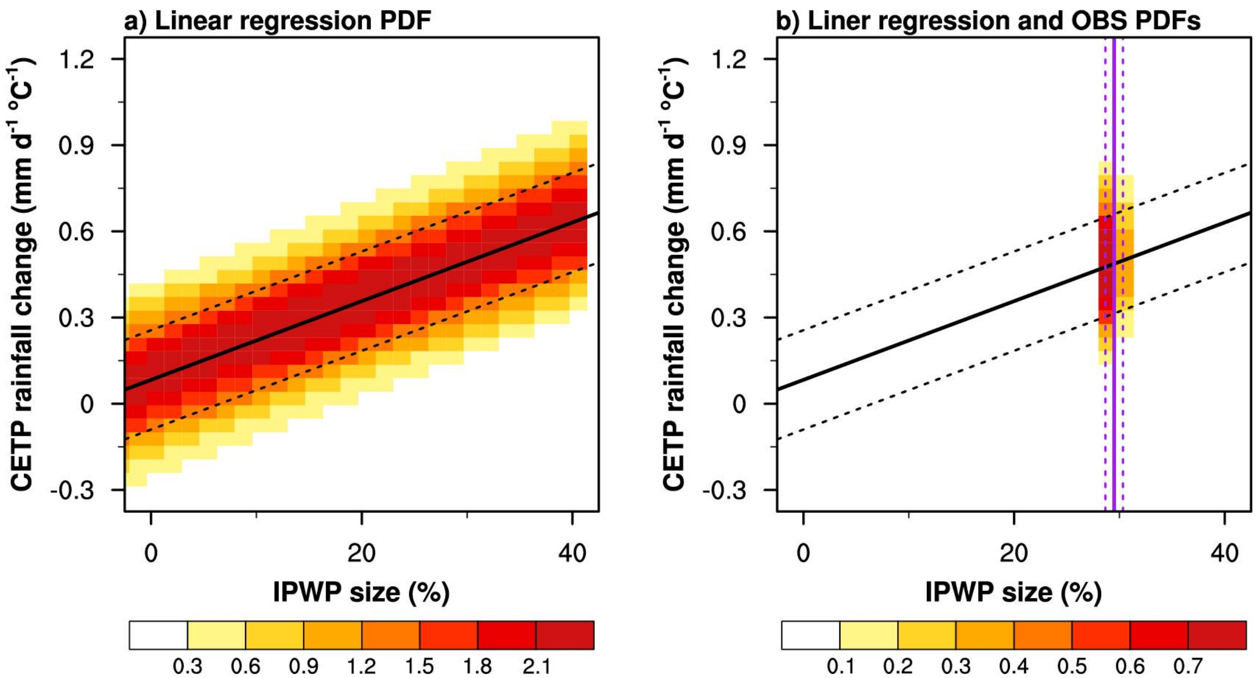

Supplementary Figure 7. The probability density function (PDF) of the emergent relationship combined with the observational constraint. a) The PDF of the linear regression between projected precipitation changes in the CETP under SSP5-8.5 and the simulated IPWP size in the present-day from 38 CMIP6 models. **b)** The PDF after emergent constraint based on observations. The solid black lines indicate the linear regression of CMIP6 models and the dashed black lines provide the prediction error (1 standard deviation, 68% confidence intervals). A solid purple line (shading) indicates the average (1 standard deviation) of observed IPWP sizes among three datasets (HadISST, ERSST, and COBE SST).

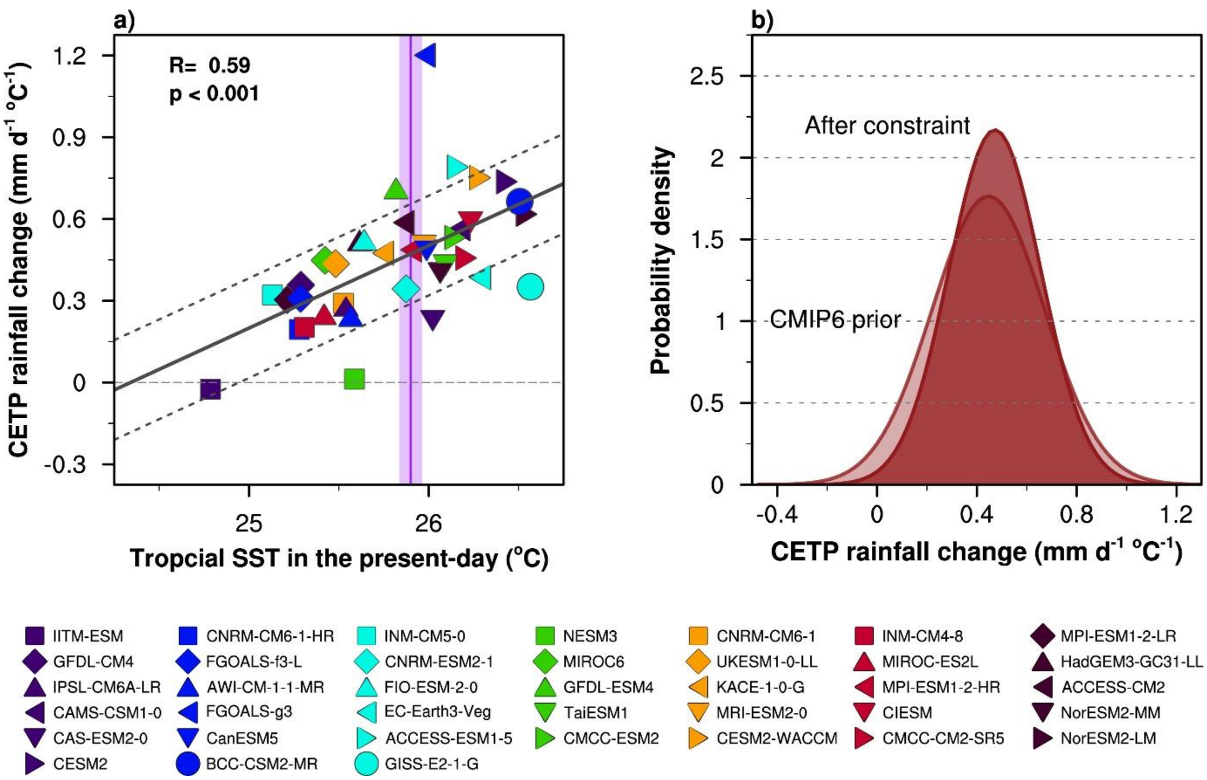

Supplementary Figure 8. Emergent constraints on the central-to-eastern tropical Pacific (CETP) precipitation changes in CMIP6. a) Projected precipitation changes in the CETP under SSP5-8.5 across the CMIP6 models versus the Tropical mean SST in the present-day (1950–1999). The solid black line follows the linear regression of 38 CMIP6 models, while the dashed black lines indicate prediction errors with one-standard deviation (68% confidence intervals). A solid purple line (shading) indicates the average (one-standard deviation) of the observed IPWP size among three datasets: HadISST, ERSSTv5, and COBE-SST2. **b)** Probability density functions for the projected precipitation changes in the CETP under SSP5-8.5, before (“CMIP6 prior”, transparent) and after (“after constraint”, opaque) the emergent constraint is applied.

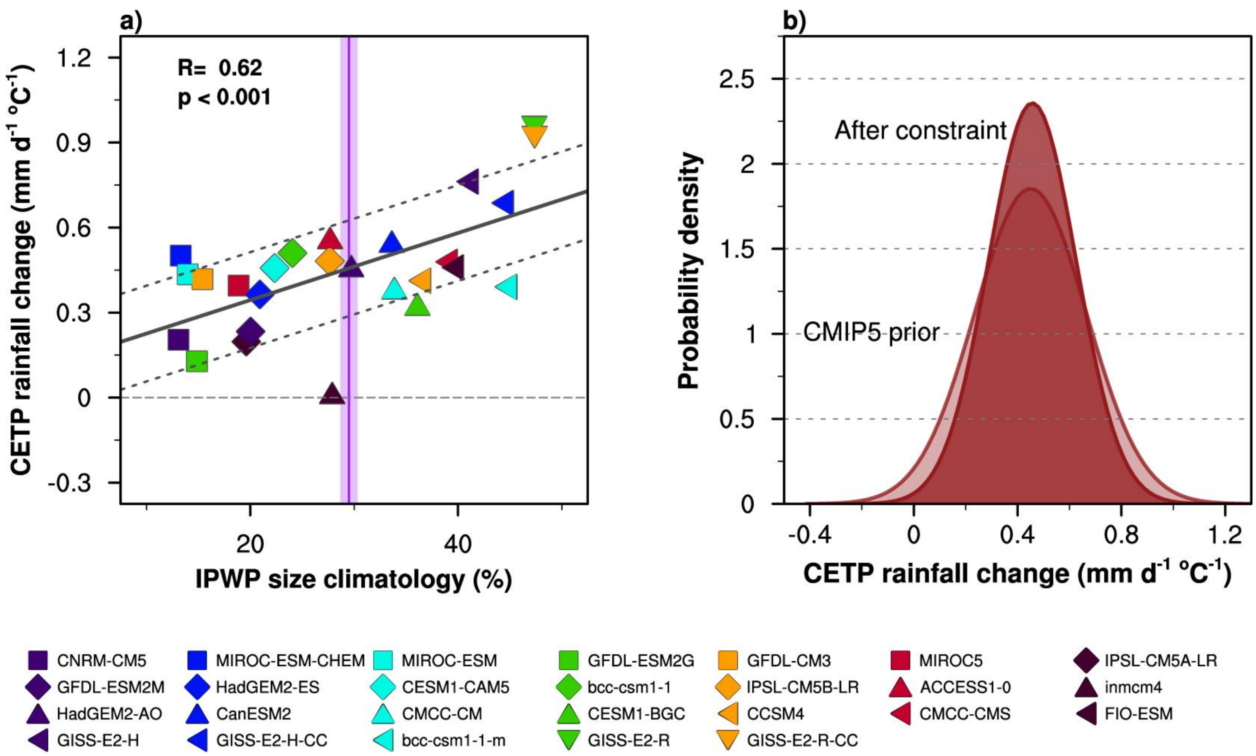

Supplementary Figure 9. Emergent constraints on the Central Pacific precipitation changes in CMIP5. a) Projected precipitation changes in the CETP across the CMIP5 models versus the Indo-Pacific warm pool (IPWP) size in the present-day (1950–1999) under RCP8.5. The solid black line indicates the linear regression of the CMIP5 models, and the dashed black lines indicate the prediction errors (68% confidence intervals). A solid purple line (shading) indicates the average (1 standard deviation) of observed IPWP sizes among three datasets (HadISST, ERSST, and COBE SST). **b)** Probability density functions for the projected precipitation changes in the CETP under RCP8.5 before (“CMIP5 prior”, transparent) and after (“after constraint”, opaque) the emergent constraint is applied.

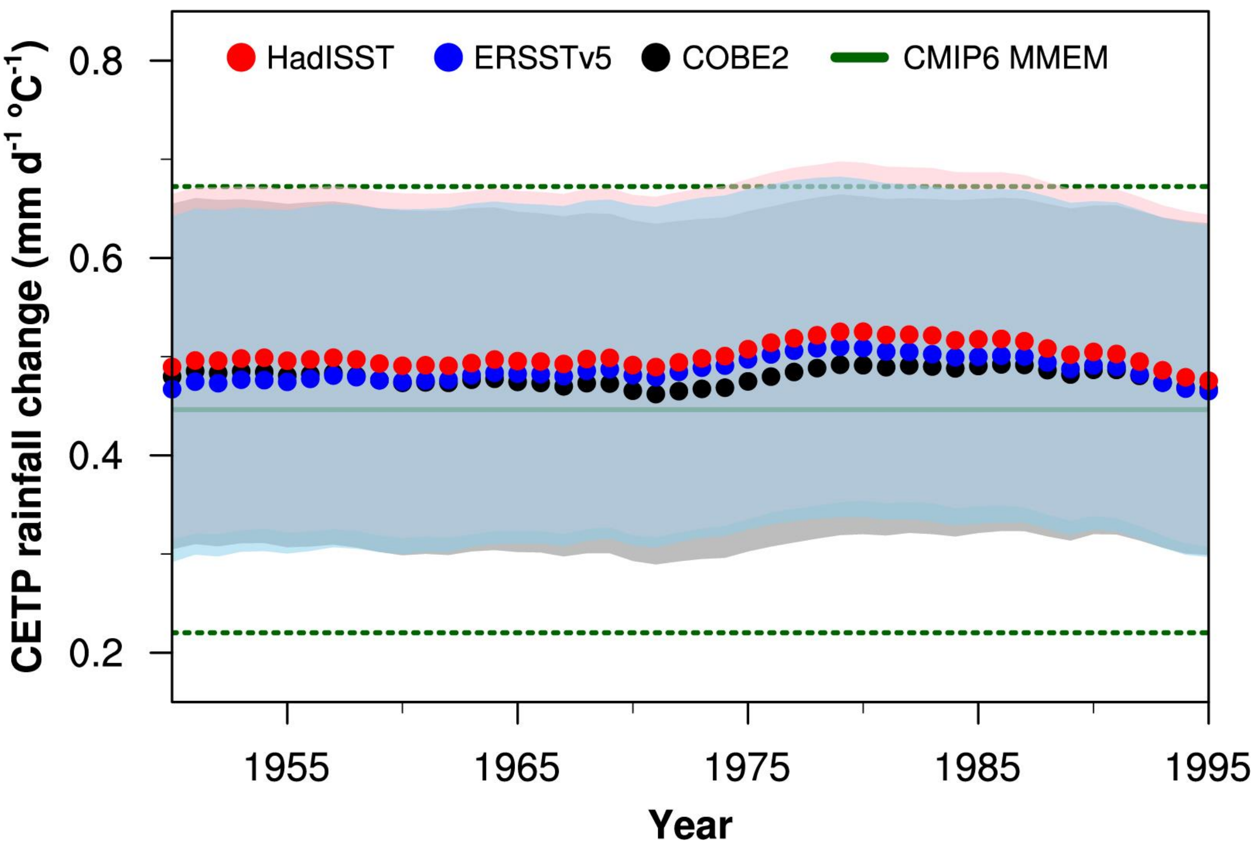

Supplementary Figure 10. Sensitivity test using independent observations and 20-year moving time-window for considering internal variabilities. Each data sets of HadISST (red), ERSSTv5(blue) and COBE2 (black) is used for observational constraint on the each 20-year moving emergent relationship. Emergent relationship among 38 models in CMIP6 is calculated by every 20-year interval and constrained by observations at same period from 1950 to 1995. Shadings indicate one-standard deviation of emergent constraints. Solid green line illustrates MMEM of future changes in CETP precipitation with unconstrained uncertainty range (dashed green lines) from inter-model one standard deviations.

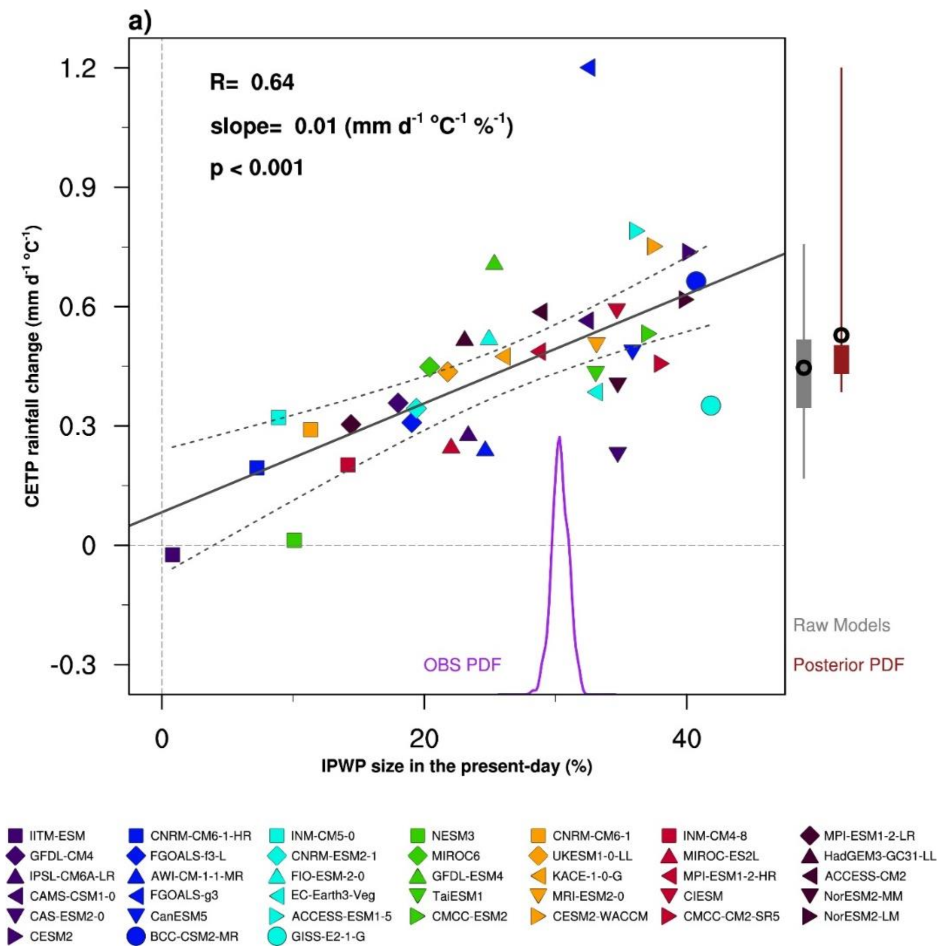

Supplementary Figure 11. Emergent constraints on the central-to-eastern tropical Pacific (CETP) precipitation changes in CMIP6 climate models using the information theoretic approach. Projected precipitation changes in the CETP under SSP5-8.5 across the CMIP6 climate models versus the Indo-Pacific warm pool (IPWP) size in the present-day (1950–1999). The solid black line follows the linear regression of 38 CMIP6 climate models, while the dashed black lines indicate prediction errors with one-standard deviation (68% confidence intervals). A solid purple line indicates the PDF of the observed IPWP size in HadISST using 200-ramdom bootstrap. The raw model spread of the future CETP changes is compared with posterior PDF using its weighted average, given the observed IPWP area in the present-day. The bars and error bars in the right y-axis indicate 66% and 90% confidence interval (one- and two- standard deviation among CMIP6 climate models with/without constraint). Circles indicate multi-model means of future precipitation changes over the CETP.

Supplementary Table 1. CMIP5 and CMIP6 models used in this study and the corresponding model center. CMIP5 models are written in italic.

Model name	**Modeling center**
ACCESS1-0 (Bi et al., 2013)	The Commonwealth Scientific and Industrial Research Organisation (Australia)
ACCESS-CM2 (Bi et al., 2020)	
ACCESS-ESM1-5 (Ziehn et al., 2020)	
AWI-CM-1-1-MR (Semmler et al., 2020)	Alfred Wegener Institute Helmholtz Centre for Polar and Marine Research (Germany)
bcc-csm1-1 (Wu et al., 2013)	Beijing Climate Center (China)
bcc-csm1-1-m (Wu et al., 2013)	
BCC-CSM2-MR (Wu et al., 2019)	
CAMS-CSM1-0 (Chen et al., 2019)	Chinese Academy of Meteorological Sciences (China)
CAS-ESM2-0 (Dong et al., 2021)	Chinese Academy of Sciences (China)
CanESM2 (Arora et al., 2011)	Canadian Centre for Climate Modelling and Analysis (Canada)
CanESM5 (Swart et al., 2019)	
CanESM5-CanOE (Swart et al., 2019)	
CCSM4 (Gent et al., 2011)	National Center for Atmospheric Research, Climate and National Center for Atmospheric Research, Climate and Global Dynamics Laboratory, (USA)
CESM1-BGC (Meehl et al., 2013)	
CESM1-CAM5 (Meehl et al., 2013)	
CESM2 (Danabasoglu et al., 2020)	
CESM2-WACCM (Danabasoglu et al., 2020)	
CMCC-CM (Scoccimarro et al., 2011)	Fondazione Centro Euro-Mediterraneo sui Cambiamenti Climatici (Italy)
CMCC-CMS (Scoccimarro et al., 2011)	
CMCC-CM2-SR5 (Cherchi et al., 2019)	
CMCC-ESM2 (Cherchi et al., 2019)	
CNRM-CM5 (Voldoire et al., 2013)	Centre National de Recherches Météorologiques (France)
CNRM-CM6-1 (Voldoire et al., 2019)	
CNRM-CM6-1-HR (Voldoire et al., 2019)	
CNRM-ESM2-1 (Voldoire et al., 2019)	

EC-Earth3-Veg (Döscher et al., 2021)	EC-Earth consortium, Rossby Center, Swedish Meteorological and Hydrological Institute/SMHI (Sweden)
FGOALS-f3-L (Li et al., 2020)	Chinese Academy of Sciences (China)
FGOALS-g3 (Li et al., 2020)	
FIO-ESM (Qiao et al., 2013)	First Institute of Oceanography, State Oceanic Administration (China)
FIO-ESM-2-0 (Bao et al., 2020)	
GFDL-CM3 (John P Dunne et al., 2012)	National Oceanic and Atmospheric Administration, Geophysical Fluid Dynamics Laboratory (USA)
GFDL-ESM2G (John P Dunne et al., 2012)	
GFDL-ESM2M (John P Dunne et al., 2012)	
GFDL-CM4 (Held et al., 2019)	
GFDL-ESM4 (J. P. Dunne et al., 2020)	
GISS-E2-H (Schmidt et al., 2014)	Goddard Institute for Space Studies, National Aeronautics and Space Administration (USA)
GISS-E2-H-CC (Schmidt et al., 2014)	
GISS-E2-R (Schmidt et al., 2014)	
GISS-E2-R-CC (Schmidt et al., 2014)	
GISS-E2-1-G (Kelley et al., 2020)	
HadGEM2-ES (Collins et al., 2011)	Met Office Hadley Centre (UK)
HadGEM3-GC31-LL (Williams et al., 2018)	
UKESM1-0-LL (Sellar et al., 2020)	
IITM-ESM(Swapna et al., 2018)	Center for Climate Change Research, Indian Institute of Tropical Meteorology Pune (India)
INM-CM4 (Volodin et al., 2010)	Institute for Numerical Mathematics, Russian Academy of Science, Moscow (Russia)
INM-CM4-8 (Volodin et al., 2018)	
INM-CM5-0 (Volodin et al., 2017)	
IPSL-CM5A-LR (Dufresne et al., 2013)	Institut Pierre-Simon Laplace (France)
IPSL-CM5A-MR (Dufresne et al., 2013)	
IPSL-CM6A-LR (Boucher et al., 2020)	
HadGEM2-AO (Baek et al., 2013)	National Institute of Meteorological Sciences/Korea Meteorological Administration, Climate Research Division (Republic of Korea)
KACE-1-0-G (Lee et al., 2020)	
MIROC5 (Watanabe et al., 2011)	Japan Agency for Marine-Earth Science and

MIROC-ESM (Watanabe et al., 2011)	Technology (Japan)
MIROC-ESM-CHEM (Watanabe et al., 2011)	
MIROC-ES2L (Hajima et al., 2020)	
MIROC6 (Tatebe et al., 2019)	
MPI-ESM-1-2-HR (Müller et al., 2018)	Max Planck Institute for Meteorology (Germany)
MPI-ESM1-2-LR (Mauritsen et al., 2019)	
MRI-ESM2-0 (Yukimoto et al., 2019)	Meteorological Research Institute (Japan)
NESM3 (Cao et al., 2018)	Nanjing University of Information Science and Technology (China)
NorESM2-LM (Seland et al., 2020)	Climate modeling Consortium consisting of Center for International Climate and Environmental Research (Norway)
NorESM2-MM (Seland et al., 2020)	
TaiESM1 (Wang et al., 2021)	Research Center for Environmental Changes, Academia Sinica (Taiwan)

Supplementary references

Arora, V. K., J. F. Scinocca, G. J. Boer, J. R. Christian, K. L. Denman, G. M. Flato, V. V. Kharin, W. G. Lee, and W. J. Merryfield Carbon emission limits required to satisfy future representative concentration pathways of greenhouse gases. *Geophysical Research Letters* ***38*** (2011). https://doi.org/10.1029/2010GL046270

Baek, H.-J., et al. Climate change in the 21st century simulated by HadGEM2-AO under representative concentration pathways. *Asia-Pac J Atmos Sci* ***49*****(5)**, 603-618 (2013). https://doi.org/10.1007/s13143-013-0053-7

Bao, Y., Z. Y. Song, and F. L. Qiao FIO-ESM Version 2.0: Model Description and Evaluation. *J Geophys Res-Oceans* ***125*****(6)**, e2019JC016036 (2020). https://doi.org/10.1029/2019JC016036

Bi, D. H., et al. Configuration and spin-up of ACCESS-CM2, the new generation Australian Community Climate and Earth System Simulator Coupled Model. *J So Hemisph Earth* **_70_(1)**, 225-251 (2020). https://doi.org/10.1071/ES19040

Bi, D. H., et al. The ACCESS coupled model: description, control climate and evaluation. *Aust Meteorol Ocean* **_63_(1)**, 41-64 (2013). https://doi.org/10.22499/2.6301.004

Boucher, O., et al. Presentation and Evaluation of the IPSL-CM6A-LR Climate Model. *J Adv Model Earth Sy* **_12_(7)**, e2019MS002010 (2020). https://doi.org/10.1029/2019MS002010

Cao, J., B. Wang, Y. M. Yang, L. B. Ma, J. Li, B. Sun, Y. Bao, J. He, X. Zhou, and L. G. Wu The NUIST Earth System Model (NESM) version 3: description and preliminary evaluation. *Geosci Model Dev* **_11_(7)**, 2975-2993 (2018). https://doi.org/10.5194/gmd-11-2975-2018

Chen, X. L., Z. Guo, T. J. Zhou, J. Li, X. Y. Rong, Y. F. Xin, H. M. Chen, and J. Z. Su Climate Sensitivity and Feedbacks of a New Coupled Model CAMS-CSM to Idealized CO2 Forcing: A Comparison with CMIP5 Models. *J Meteorol Res-Prc* **_33_(1)**, 31-45 (2019). https://doi.org/10.1007/s13351-019-8074-5

Cherchi, A., et al. Global Mean Climate and Main Patterns of Variability in the CMCC-CM2 Coupled Model. *J Adv Model Earth Sy* **_11_(1)**, 185-209 (2019). https://doi.org/10.1029/2018MS001369

Collins, W. J., et al. Development and evaluation of an Earth-System model – HadGEM2. *Geosci. Model Dev.* **_4_(4)**, 1051-1075 (2011). https://doi.org/10.5194/gmd-4-1051-2011

Danabasoglu, G., et al. The Community Earth System Model Version 2 (CESM2). *J Adv Model Earth Sy* **_12_(2)**, e2019MS001916 (2020). https://doi.org/10.1029/2019MS001916

Dong, X., et al. CAS-ESM2.0 Model Datasets for the CMIP6 Ocean Model Intercomparison Project Phase 1 (OMIP1). *Adv Atmos Sci* ***38*****(2)**, 307-316 (2021). https://doi.org/10.1007/s00376-020-0150-3

Döscher, R., M. Acosta, A. Alessandri, P. Anthoni, A. Arneth, T. Arsouze, T. Bergmann, R. Bernadello, S. Bousetta, and L.-P. J. G. M. D. D. Caron The EC-earth3 Earth system model for the climate model intercomparison project 6. *Geoscientific Model Development Discussions* (2021). https://doi.org/10.5194/gmd-2020-446

Dufresne, J. L., et al. Climate change projections using the IPSL-CM5 Earth System Model: from CMIP3 to CMIP5. *Clim Dynam* ***40*****(9-10)**, 2123-2165 (2013). https://doi.org/10.1007/s00382-012-1636-1

Dunne, J. P., J. G. John, A. J. Adcroft, S. M. Griffies, R. W. Hallberg, E. Shevliakova, R. J. Stouffer, W. Cooke, K. A. Dunne, and M. J. J. J. o. c. Harrison GFDL's ESM2 global coupled climate–carbon earth system models. Part I: Physical formulation and baseline simulation characteristics. *Journal of Climate* ***25*****(19)**, 6646-6665 (2012). https://doi.org/10.1175/JCLI-D-11-00560.1

Dunne, J. P., et al. The GFDL Earth System Model Version 4.1 (GFDL-ESM 4.1): Overall Coupled Model Description and Simulation Characteristics. *J Adv Model Earth Sy* ***12*****(11)**, e2019MS002015 (2020). https://doi.org/10.1029/2019MS002015

Gent, P. R., et al. The Community Climate System Model Version 4. *Journal of Climate* ***24*****(19)**, 4973-4991 (2011). https://doi.org/10.1175/2011JCLI4083.1

Hajima, T., et al. Development of the MIROC-ES2L Earth system model and the evaluation of biogeochemical processes and feedbacks. *Geosci Model Dev* ***13*****(5)**, 2197-2244 (2020). https://doi.org/10.5194/gmd-13-2197-2020

Held, I. M., et al. Structure and Performance of GFDL's CM4.0 Climate Model. *J Adv Model Earth Sy* ***11*****(11)**, 3691-3727 (2019). https://doi.org/10.1029/2019MS001829

Kelley, M., et al. GISS-E2.1: Configurations and Climatology. *J Adv Model Earth Sy* ***12*****(8)**, e2019MS002025 (2020). https://doi.org/10.1029/2019MS002025

Lee, J., J. Kim, M. A. Sun, B. H. Kim, H. Moon, H. M. Sung, J. Kim, and Y. H. Byun Evaluation of the Korea Meteorological Administration Advanced Community Earth-System model (K-ACE). *Asia-Pac J Atmos Sci* ***56*****(3)**, 381-395 (2020). https://doi.org/10.1007/s13143-019-00144-7

Mauritsen, T., et al. Developments in the MPI-M Earth System Model version 1.2 (MPI-ESM1.2) and Its Response to Increasing CO2. *J Adv Model Earth Sy* ***11*****(4)**, 998-1038 (2019). https://doi.org/10.1029/2018MS001400

Meehl, G. A., W. M. Washington, J. M. Arblaster, A. X. Hu, H. Y. Teng, J. E. Kay, A. Gettelman, D. M. Lawrence, B. M. Sanderson, and W. G. Strand Climate Change Projections in CESM1(CAM5) Compared to CCSM4. *Journal of Climate* ***26*****(17)**, 6287-6308 (2013). https://doi.org/10.1175/JCLI-D-12-00572.1

Müller, W. A., J. H. Jungclaus, T. Mauritsen, J. Baehr, M. Bittner, R. Budich, F. Bunzel, M. Esch, R. Ghosh, and H. J. J. o. A. i. M. E. S. Haak A higher-resolution version of the Max Planck institute earth system model (MPI-ESM1. 2-HR). *J Adv Model Earth Sy* ***10*****(7)**, 1383-1413 (2018). https://doi.org/10.1029/2017MS001217

Qiao, F. L., Z. Y. Song, Y. Bao, Y. J. Song, Q. Shu, C. J. Huang, and W. Zhao Development and evaluation of an Earth System Model with surface gravity waves. *J Geophys Res-Oceans* ***118*****(9)**, 4514-4524 (2013). https://doi.org/10.1002/jgrc.20327

Schmidt, G. A., et al. Configuration and assessment of the GISS ModelE2 contributions to the CMIP5 archive. *J Adv Model Earth Sy* ***6*****(1)**, 141-184 (2014). https://doi.org/10.1002/2013MS000265

Scoccimarro, E., S. Gualdi, A. Bellucci, A. Sanna, P. G. Fogli, E. Manzini, M. Vichi, P. Oddo, and A. Navarra Effects of Tropical Cyclones on Ocean Heat Transport in a High-Resolution Coupled General Circulation Model. *Journal of Climate* ***24*****(16)**, 4368-4384 (2011). https://doi.org/10.1175/2011JCLI4104.1.

Seland, O., et al. Overview of the Norwegian Earth System Model (NorESM2) and key climate response of CMIP6 DECK, historical, and scenario simulations. *Geosci Model Dev* ***13*****(12)**, 6165-6200 (2020). https://doi.org/10.5194/gmd-2019-378

Sellar, A. A., et al. Implementation of UK Earth System Models for CMIP6. *J Adv Model Earth Sy* ***12*****(4)**, e2019MS001946 (2020). https://doi.org/10.1029/2019MS001946

Semmler, T., et al. Simulations for CMIP6 With the AWI Climate Model AWI-CM-1-1. *J Adv Model Earth Sy* ***12*****(9)**, e2019MS002009 (2020). https://doi.org/10.1029/2019MS002009

Swapna, P., R. Krishnan, N. Sandeep, A. G. Prajeesh, D. C. Ayantika, S. Manmeet, and R. Vellore Long-Term Climate Simulations Using the IITM Earth System Model (IITM-ESMv2) With Focus on the South Asian Monsoon. *J Adv Model Earth Sy* ***10*****(5)**, 1127-1149 (2018). https://doi.org/10.1029/2017MS001262

Swart, N. C., et al. The Canadian Earth System Model version 5 (CanESM5.0.3). *Geosci Model Dev* ***12*****(11)**, 4823-4873 (2019). https://doi.org/10.5194/gmd-12-4823-2019

Tatebe, H., et al. Description and basic evaluation of simulated mean state, internal variability, and climate sensitivity in MIROC6. *Geosci Model Dev* ***12*****(7)**, 2727-2765 (2019). https://doi.org/10.5194/gmd-12-2727-2019

Voldoire, A., et al. The CNRM-CM5.1 global climate model: description and basic evaluation. *Clim Dynam* ***40*****(9-10)**, 2091-2121 (2013). https://doi.org/10.1007/s00382-011-1259-y

Voldoire, A., et al. Evaluation of CMIP6 DECK Experiments With CNRM-CM6-1. *J Adv Model Earth Sy* ***11*****(7)**, 2177-2213 (2019). https://doi.org/10.1029/2019MS001683

Volodin, E. M., N. A. Dianskii, and A. V. Gusev Simulating present-day climate with the INMCM4.0 coupled model of the atmospheric and oceanic general circulations. *Izvestiya, Atmospheric and Oceanic Physics* ***46*****(4)**, 414-431 (2010). https://doi.org/10.1134/S000143381004002X

Volodin, E. M., E. V. Mortikov, S. V. Kostrykin, V. Y. Galin, V. N. Lykossov, A. S. Gritsun, N. A. Diansky, A. V. Gusev, and N. G. Iakovlev Simulation of the present-day climate with the climate model INMCM5. *Clim Dynam* ***49*****(11-12)**, 3715-3734 (2017). https://doi.org/10.1007/s00382-017-3539-7

Volodin, E. M., et al. Simulation of the modern climate using the INM-CM48 climate model. *Russ J Numer Anal M* ***33*****(6)**, 367-374 (2018). https://doi.org/10.1515/rnam-2018-0032

Williams, K. D., et al. The Met Office Global Coupled Model 3.0 and 3.1 (GC3.0 and GC3.1) Configurations. *J Adv Model Earth Sy* ***10*****(2)**, 357-380 (2018). https://doi.org/10.1002/2017MS001115

Wu, T. W., et al. The Beijing Climate Center Climate System Model (BCC-CSM): the main progress from CMIP5 to CMIP6. *Geosci Model Dev* ***12*****(4)**, 1573-1600 (2019). https://doi.org/10.5194/gmd-12-1573-2019

Wu, T. W., et al. Global carbon budgets simulated by the Beijing Climate Center Climate System Model for the last century. *J Geophys Res-Atmos* ***118*****(10)**, 4326-4347 (2013). https://doi.org/10.1002/jgrd.50320

Yukimoto, S., et al. The Meteorological Research Institute Earth System Model Version 2.0, MRI-ESM2.0: Description and Basic Evaluation of the Physical Component. *J. Meteorol. Soc. Jpn.* ***97*****(5)**, 931-965 (2019). https://doi.org/10.2151/jmsj.2019-051

Ziehn, T., M. A. Chamberlain, R. M. Law, A. Lenton, R. W. Bodman, M. Dix, L. Stevens, Y. P. Wang, and J. Srbinovsky The Australian Earth System Model: ACCESS-ESM1.5. *J So Hemisph Earth* ***70*****(1)**, 193-214 (2020). https://doi.org/10.1071/ES19035